

# UC Davis

## UC Davis Previously Published Works

**Title**

Automatic design of synthetic gene circuits through mixed integer non-linear programming.

**Permalink**

<https://escholarship.org/uc/item/5jz8t8b7>

**Journal**

PloS one, 7(4)

**ISSN**

1932-6203

**Authors**

Huynh, Linh  
Kececioglu, John  
Köppe, Matthias  
et al.

**Publication Date**

2012

**DOI**

10.1371/journal.pone.0035529

Peer reviewed

# Automatic Design of Synthetic Gene Circuits through Mixed Integer Non-linear Programming

Linh Huynh<sup>1,2</sup>, John Kececioğlu<sup>3</sup>, Matthias Köppe<sup>4</sup>, Ilias Tagkopoulos<sup>1,2\*</sup>

**1** Department of Computer Science, University of California Davis, Davis, United States of America, **2** Genome Center, University of California Davis, Davis, California, United States of America, **3** Department of Computer Science, University of Arizona, Tucson, Arizona, United States of America, **4** Department of Mathematics, University of California Davis, Davis, California, United States of America

## Abstract

Automatic design of synthetic gene circuits poses a significant challenge to synthetic biology, primarily due to the complexity of biological systems, and the lack of rigorous optimization methods that can cope with the combinatorial explosion as the number of biological parts increases. Current optimization methods for synthetic gene design rely on heuristic algorithms that are usually not deterministic, deliver sub-optimal solutions, and provide no guarantees on convergence or error bounds. Here, we introduce an optimization framework for the problem of part selection in synthetic gene circuits that is based on mixed integer non-linear programming (MINLP), which is a deterministic method that finds the globally optimal solution and guarantees convergence in finite time. Given a synthetic gene circuit, a library of characterized parts, and user-defined constraints, our method can find the optimal selection of parts that satisfy the constraints and best approximates the objective function given by the user. We evaluated the proposed method in the design of three synthetic circuits (a toggle switch, a transcriptional cascade, and a band detector), with both experimentally constructed and synthetic promoter libraries. Scalability and robustness analysis shows that the proposed framework scales well with the library size and the solution space. The work described here is a step towards a unifying, realistic framework for the automated design of biological circuits.

**Citation:** Huynh L, Kececioğlu J, Köppe M, Tagkopoulos I (2012) Automatic Design of Synthetic Gene Circuits through Mixed Integer Non-linear Programming. PLoS ONE 7(4): e35529. doi:10.1371/journal.pone.0035529

**Editor:** Mukund Thattai, Tata Institute of Fundamental Research, India

**Received:** August 9, 2011; **Accepted:** March 16, 2012; **Published:** April 20, 2012

**Copyright:** © 2012 Huynh et al. This is an open-access article distributed under the terms of the Creative Commons Attribution License, which permits unrestricted use, distribution, and reproduction in any medium, provided the original author and source are credited.

**Funding:** The authors would like to acknowledge support from grant 0941360 and 1146926 from the National Science Foundation. LH is supported by the Vietnam Education Foundation fellowship. The funders had no role in study design, data collection and analysis, decision to publish, or preparation of the manuscript.

**Competing Interests:** The authors have declared that no competing interests exist.

\* E-mail: itagkopoulos@ucdavis.edu

## Introduction

Synthetic biology is a nascent field with transformative potential to a variety of disciplines, ranging from development of therapeutics [1] to biofuel production [2]. Although automation is one of the conceptual pillars of synthetic biology, designs still rely on a trial-and-error and tinkering approaches. When it comes to automated biological circuit design, computer-aided design (CAD) tools have still low penetrance to biological circuit design despite notable developments in the field. Recent advances include efforts to adapt electrical engineering concepts, such as Boolean optimization and Carnaugh maps, to biological circuit design of digital functions [3], and approaches that build formal high-level languages to translate from user-defined specifications to genetic circuits that adhere to digital logic [4], [5], [6].

In the realm of analog synthetic gene design, heuristic methods such as evolutionary algorithms [7], [8] and simulated annealing [9] were employed. Relevant approaches include the exploration of the functionality space of a given library [10], library-agnostic robustness analysis to determine what mutation sites for achieving the desired functionality [11]. Notably, a deterministic optimization framework was proposed by Dasika and Manaras [12] to find synthetic constructs by using an outer approximation procedure. Despite its novelty, the capabilities of that method are limited, as it targets only steady-state problems and it cannot guarantee

optimality in non-convex problems, which usually is the case in biological systems.

In this paper, we focus on the problem of optimal part selection: given a library of biological parts, an objective function (e.g. a desired temporal protein profile or a dose-dependent protein expression profile), user-defined constraints (e.g. the maximum number of coding regions per promoter), and an existing abstract circuit topology, we try to find the optimal set of parts from the library so that the final circuit best approximates the objective function, given the constraints. An overview of the proposed optimization framework is illustrated in figure 1.

## Methods

### Nonlinear Model

We first describe a non-linear model that incorporates regulation, degradation, transcription and translation, and allows multiple gene copies with distinct regulation to be present in the genetic circuit. Let  $pro(i)$  be the set of all promoters that are upstream of the one or more copies of gene  $i$ . The various promoters may include transcription factor binding sites (TFBS) that will be part of the *cis*-regulatory region of a gene. For each promoter  $k$  in  $pro(i)$  the (possibly empty) sets  $act(k)$  and  $rep(k)$  contain all activator and repressor proteins that are present in promoter  $k$ , respectively. Using Hill equations (see [13], [14], [15]

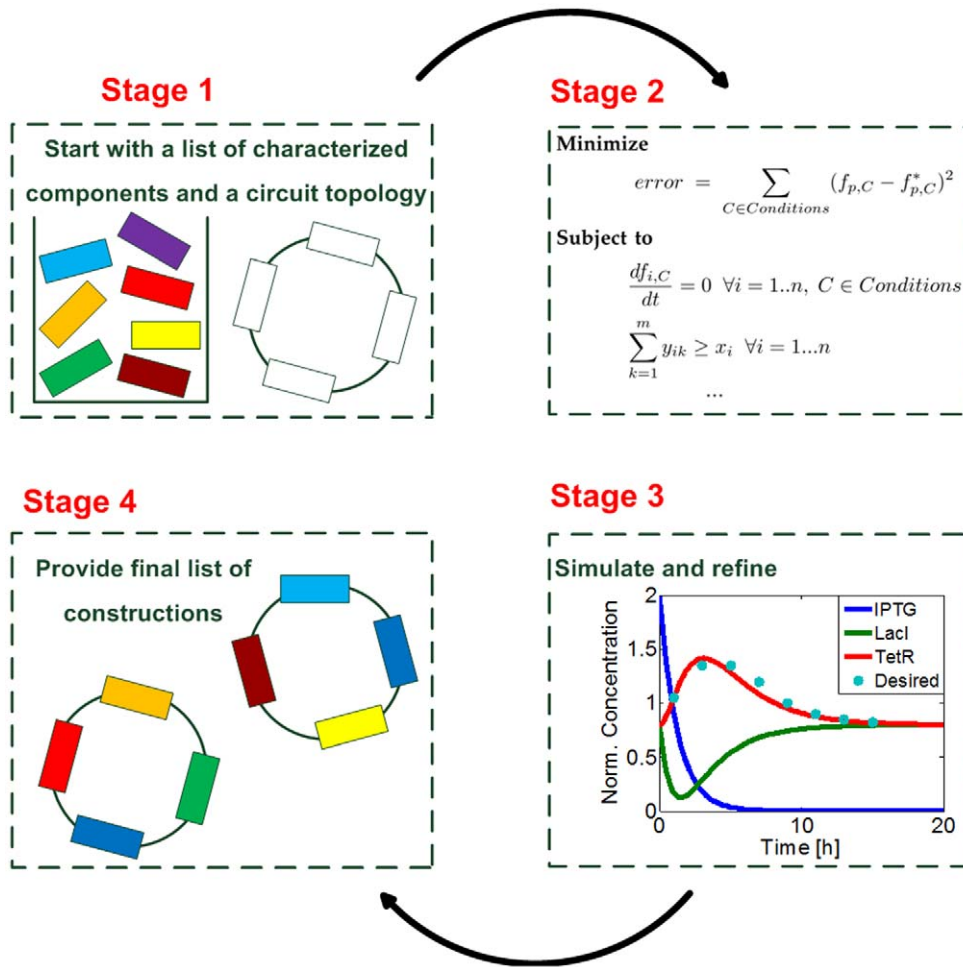


**Figure 1. System overview of the proposed optimization framework.** The software requires access to a library of characterized parts (such as a subset of the parts available in Parts Registry) that will be used as fundamental blocks in the synthetic circuit. The user will have to supply a specific design (static connectivity), together with a set of constraints and a specific objective function to be optimized. The software will translate this system to a set of linear constraints that it will subsequently solve. The result of the optimization framework will be the set of parts that have to be used, and at what position. The system will have the ability to simulate the proposed design, and provide candidate synthetic circuits for experimental construction in the laboratory.

doi:10.1371/journal.pone.0035529.g001

and [16]), the concentration of protein  $i$  can be modeled as an ordinary differential equation (ODE) as follows:

$$\frac{df_i}{dt} = \sum_{k \in pro(i)} (\alpha_{0k} + \alpha_k \prod_{a \in act(k)} \frac{\beta_{ak} f_a^{\eta_{ak}}}{1 + \beta_{ak} f_a^{\eta_{ak}}}) - (d_i + \mu) f_i \quad (1)$$

where  $f_i(t)$ ,  $f_a(t)$  and  $f_r(t)$  are the concentration at time point  $t$  of proteins  $i$ ,  $a$  and  $r$ , respectively. For each promoter  $k$  in  $pro(i)$ ,  $\alpha_{0k}$  and  $\alpha_k$  are its basal production and protein synthesis coefficient,  $\eta_{ak}$  and  $\eta_{rk}$  are the cooperativity coefficients for activator  $a$  and repressor  $r$ ,  $\beta_{ak}$  and  $\beta_{rk}$  are the binding affinities of activator  $a$  and repressor  $r$ . The degradation of protein  $i$  is captured by parameter  $d_i$ . The growth rate is represented with  $\mu$ , and it is considered to be zero in stationary phase.

In many cases, gene expression is controlled by exogenously applied chemicals that induce gene expression through molecular binding. We can incorporate the effect of inducers by explicitly modeling the total amount of any protein  $j$  in the cell as the sum of

the free ( $f_j^{free}$ ) and inducer-bound protein ( $f_j^{bound}$ ), which results in the following Hill equation model:

$$f_j = f_j^{free} + f_j^{bound}, \quad (2)$$

$$f_j^{free} = \frac{\theta^n f_j}{\theta^n + [inducer]^\eta}, \quad (3)$$

$$f_j^{bound} = \frac{[inducer]^\eta f_j}{\theta^n + [inducer]^\eta}, \quad (4)$$

where  $[inducer]$  is the inducer concentration,  $\eta$  is the Hill coefficient (cooperativity factor) and  $\theta$  is the dissociation constant. Note that equations 2 to 4 apply for both activators and repressors, and in cases where binding of the inducer renders the transcription factor either active or inactive. For example, when inducer binding to the transcriptor factor activates transcription (as it is the case with AraC and arabinose), then the activator concentration  $f_a$  in the RHS of equation 1 is given by  $f_a^{bound}$  from equation 4.

Equation 1 provides a non-linear representation of protein concentration, which can be combined with binary variables that correspond to the presence/absence of a specific promoter in the synthetic circuit to formulate an optimization design problem. We introduce the following equation to express the concentration of protein  $i$  as a function of the available promoters and proteins:

$$\frac{df_i}{dt} = \sum_{k=1}^m y_{ik} (\alpha_{0k} + \alpha_k \prod_{a \in \text{act}(k)} \frac{\beta_{ak} f_a^{\eta_{ak}}}{1 + \beta_{ak} f_a^{\eta_{ak}}}) \prod_{r \in \text{rep}(k)} \frac{1}{1 + \beta_{rk} f_r^{\eta_{rk}}} - (d_i + \mu) f_i, \quad (5)$$

where  $m$  is the number of all promoters and binary variables  $y_{ik}$  represent the presence or absence of promoter  $k$  upstream of gene  $i$ :

$$y_{ik} = \begin{cases} 1 & \text{if promoter } k \text{ is up stream} \\ & \text{of protein } i \\ 0 & \text{otherwise.} \end{cases} \quad (6)$$

### Linear Model

The non-linear model formulation works well when the objective function is to approximate a *steady-state* expression profile since setting the derivative in equation 1 to zero results in a polynomial equation. However, approximating temporal profiles through a system of non-linear differential equations that incorporate integer variables (e.g.,  $y_{ik}$ ) lead to a mixed integer dynamic optimization (MIDO) problem, which cannot be solved efficiently [17].

To overcome this challenge, we introduce a linearization of the non-linear model that was given in (5) by using a linear approximation around a steady-state point [18]. Approximating the model through taking the first terms of its Taylor expansion, and then incorporating the binary selection variables  $y_{ik}$  that we introduced in eq. 6 yields:

$$\frac{df_i}{dt} = \sum_{k=1}^m y_{ik} (\gamma_k + \sum_{a \in \text{act}(k)} K_{ak} f_a - \sum_{r \in \text{rep}(k)} K_{rk} f_r) - (d_i + \mu) f_i \quad (7)$$

where  $K_{ak}, K_{rk}$  are coefficients of first order terms in the Taylor expansion over variables  $f_a$  and  $f_r$  in equation 5, and  $\gamma_k$  is the residual constant. Assuming  $m$  promoters and  $n$  proteins total in the library, we can reformulate the above expression (eq. 7) by introducing the parameter  $a_{ijk}$  as the regulatory effect of protein  $j$  to the expression of gene  $i$  when  $j$  is bound on the upstream promoter  $k$  of  $i$  (i.e.,  $a_{ijk} = K_{jk}$  if  $j$  is an activator of  $k$ ,  $a_{ijk} = -K_{jk}$  if  $j$  is a repressor of  $k$ , and  $a_{ijk} = 0$  if  $j$  is neither an activator nor a repressor of  $k$ ):

$$\frac{df_i}{dt} = \sum_{k=1}^m \sum_{j=1}^n y_{ik} a_{ijk} f_j - (d_i + \mu) f_i + b_i \quad (8)$$

where

$$b_i = \sum_{k=1}^m y_{ik} \gamma_k \quad (9)$$

Equation 8 described the protein production rate for any protein in a closed protein set  $f = (f_1, f_2, \dots, f_n)$ . To solve this linear system, we re-write it in its matrix form, as follows:

$$\dot{f} = Af + b \quad (10)$$

where the elements of the  $A$  matrix are defined as:

$$A_{ij} = \begin{cases} \sum_{k=1}^m a_{ijk} y_{ik} & \text{if } i \neq j \\ \sum_{k=1}^m a_{ijk} y_{ik} - d_i - \mu & \text{if } i = j \end{cases} \quad (11)$$

and  $b$  is given by

$$b = (b_1, b_2, \dots, b_n)^T$$

Assuming that matrix  $A$  is invertible, the analytical solution of this equation is as follows [19]:

$$f = e^{At} (f_0 + A^{-1}b) - A^{-1}b, \quad (12)$$

where  $f_0 = (f_1^0, f_2^0, \dots, f_n^0)$  are the initial concentrations of the proteins  $f_i$  in the closed set  $f$ . In cases where matrix  $A$  can be diagonalized, then the term  $e^{At}$  in equation 12 is given by:

$$e^{At} = SDS^{-1}, \quad (13)$$

where  $S$  is the matrix which columns are the eigenvectors of  $A$ , each corresponding to a distinct eigenvalue  $\lambda_i$ , and  $D$  is the diagonal matrix, where the diagonal elements are equal to  $e^{\lambda_i t}$ . The diagonalization of matrix  $A$  can be achieved in many special cases (e.g., when the characteristic polynomial is simple, the eigenvalues can be explicitly calculated). For the scenarios when this is not feasible, we can approximate  $e^{At}$  by taking its Taylor expansion, although this can be computationally intensive if high accuracy is needed [20]:

$$e^{At} = \sum_{i=0}^{\infty} \frac{(At)^i}{i!} \quad (14)$$

The linearization of the non-linear model, as described in this section, provides an efficient method to approximate non-linear temporal dynamics. However, it may perform poorly when the dynamics of the system to optimize are highly non-linear (oscillatory behavior, bi-stability, etc.). In such cases, we can divide the desired temporal profile into multiple domains/intervals, under which the linear system can better approximate the non-linear dynamics. By solving the optimization problem over multiple intervals, the algorithm is able to compute candidate solutions with higher accuracy, at the cost of higher time and space complexity. To ensure continuity during optimization of calculated protein concentration in successive intervals, the initial concentration  $f_i^0$  of protein  $i$  at any interval can be set to be equal to the final protein concentration in the preceding interval. In this paper, we use this setup for the temporal profile optimization of the toggle switch design.

### Steady state optimization

In the case of steady-state optimization, our task is to design a genetic circuit in which one or more proteins operate at a specific concentration values, that may be given as a function of an exogenous parameter (e.g., inducer concentration). In the context of MINLP, the formulation of the problem is as follows:

#### Minimize

**Table 1.** Parameter values.

Description	Notation	Min	Max	Value	Units	References
Duality gap threshold (COUENNE)	$\varepsilon$	$10^{-5}$	$10^{-15}$			
Protein synthesis coefficient						
Constitutive promoters	$\alpha_{pCONST}$	0.1	25.5		au/h	[27] [30]
LAC promoters	$\alpha_{pLAC}$	0.3	7.1		au/h	[26] [30] [23]
TET promoters	$\alpha_{pTET}$	0.3	9.2		au/h	[26] [30]
BAD promoters	$\alpha_{pBAD}$	2.8	3.4		au/h	[28]
Basal production						
LAC promoters	$\alpha_{0pLAC}$	0.003	0.2		au/h	[26] [30]
TET promoters	$\alpha_{0pTET}$	0.003	0.03		au/h	[26]
BAD promoters	$\alpha_{0pBAD}$	0.002	0.005		au/h	[28]
Binding affinity						
LacI & LAC promoter	$\beta_{LacI-pLAC}$			1296	$\text{au}^{-2}$	[30]
CRP & LAC promoter	$\beta_{CRP-pLAC}$			27	$\text{au}^{-1}$	[31]
TetR & TET promoter	$\beta_{TetR-pTET}$			720	$\text{au}^{-2}$	[30]
AraC & BAD promoter	$\beta_{AraC-pBAD}$			10800	$\text{au}^{-2}$	[28]
Cooperativity coefficient						
LacI	$\eta_{LacI-pLAC}$			2		[23]
CRP	$\eta_{CRP-pLAC}$			1		[31]
TetR	$\eta_{TetR-pTET}$			2		[32]
AraC	$\eta_{AraC-pBAD}$			2		[12]
IPTG	$\eta_{IPTG-LacI}$			2		[25]
aTc	$\eta_{aTc-TetR}$			2		[25]
L-arabinose	$\eta_{Larabinose-AraC}$			2		[28]
Degradation rate						
LacI	$d_{LacI}$	0.9	8.3	0.9	1/h	[33] [23] [30]
TetR	$d_{TetR}$	1.5	8.3	1.5	1/h	[33] [30]
AraC	$d_{AraC}$			0.69	1/h	[34]
CRP	$d_{CRP}$			0.7	1/h	[35]
GFP	$d_{GFP}$	0.7	4.2	1.04	1/h	[36] [23]
yEFP	$d_{yEFP}$			0.9	1/h	[30]
Dissociation constant						
IPTG	$\theta_{IPTG-LacI}$			30	$\mu\text{M}$	[25]
aTc	$\theta_{aTc-TetR}$			26.3	$\mu\text{M}$	[8]
L-arabinose	$\theta_{Larabinose-AraC}$			2.8	$\mu\text{M}$	[28]

Parameter values that were used for the evaluation, and literature reference where they are reported. In the case where values are normalized, arbitrary units ("au") are used.

doi:10.1371/journal.pone.0035529.t001

$$\text{error} = \sum_{C \in \text{Conditions}} (f_{p,C} - f_{p,C}^*)^2 \quad (15)$$

$$\sum_{k=1}^m y_{ik} \leq M_1 x_i \quad \forall i = 1, \dots, n \quad (18)$$

**Subject to**

$$\frac{df_{i,C}}{dt} = 0 \quad \forall i = 1, \dots, n, C \in \text{Conditions} \quad (16)$$

$$\sum_{i=1}^n y_{ik} \leq M_2 \quad \forall k = 1, \dots, m, \quad (19)$$

$$\sum_{k=1}^m y_{ik} \geq x_i \quad \forall i = 1, \dots, n \quad (17)$$

where *Conditions* is the set of the desired input/output value pairs that are given,  $f_{p,C}$  and  $f_{p,C}^*$  are the estimated and the desired steady state concentration of a protein  $p$  in condition  $C$ , respectively. The binary variable  $x_i$  captures the presence or

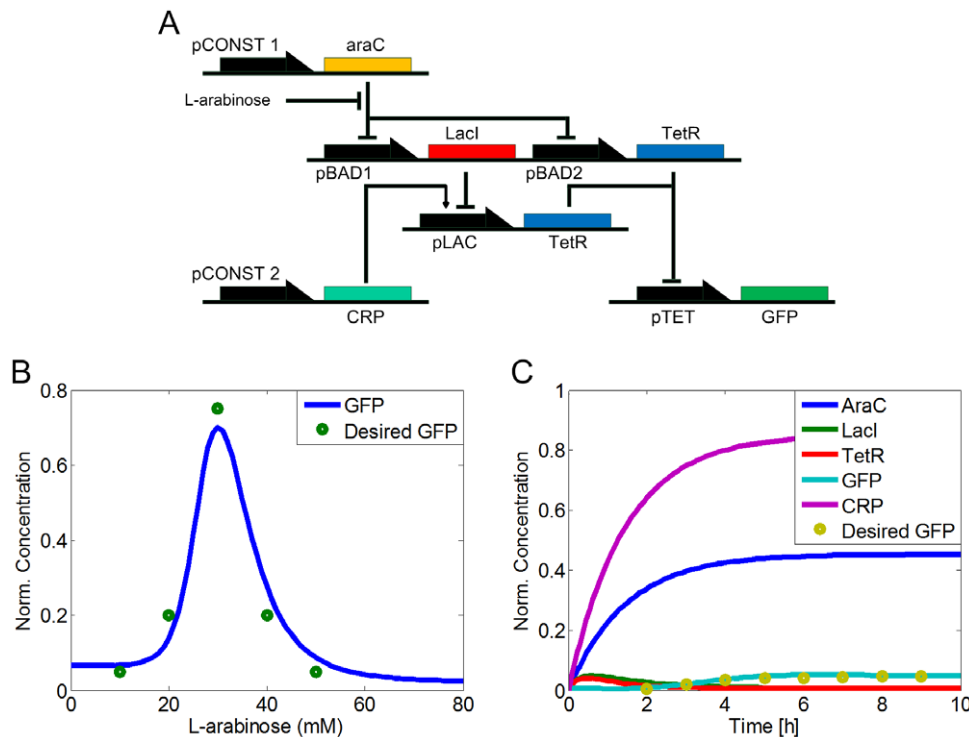


**Figure 2. Band-pass filter design.** A) The system will only express the reporter when the concentration of the input signal (L-arabinose) is in a specific range. In this design, pCONST1 and pCONST2 are constitutive promoters, while pBAD1, pBAD2 and pLAC are the promoters where AraC and LacI bind, respectively. There are two coding regions of TetR which are put on the downstream of promoters pBAD2 and pLAC. In the absence of L-arabinose, AraC activates TetR production by de-repressing the pLAC promoter. In high L-arabinose concentrations, TetR is again produced through the de-repression of the pBAD2 promoter. In significant, but not high inducer concentrations, however, none of the pathways are active enough, which in turn results in lower TetR levels and subsequent expression of the reporter GFP output. B) Reporter protein concentration (output) versus L-arabinose levels (input). The output of the synthetic circuit becomes high only at moderate values of L-arabinose. Green circles denote desired values (fluorescence measurements) that act as input to our optimization platform. C) Temporal expression profile of the band-pass filter. Temporal profile of the resulting optimal synthetic gene circuit, for a L-arabinose level of 30 mM. The GFP concentration of the optimization-derived circuit (cyan solid line) matches well the desired input values (yellow solid dots). doi:10.1371/journal.pone.0035529.g002

absence of gene  $i$  in the circuit.  $M_1$  and  $M_2$  are the maximum number of promoters at the upstream of each gene copy, and the maximum number of genes downstream of each promoter, respectively. The first constraint (eq. 16) represents the steady state condition by setting the LHS of equation 5 to be zero for all conditions (e.g., different inducer concentrations). The next two constraints ensure that there will be at least one promoter for each gene (eq. 17), but none for a gene that is not a part of the genetic circuit (eq. 18). The last constraint is optionally given by the user and it is used to limit the maximum number of genes in an operon (eq. 19).

### Temporal profile optimization

In the case of finding the components of the genetic circuit that best approximates a temporal profile, the MINLP problem is formulated as follows:

#### Minimize

$$\text{error} = \sum_{t \in T} (f_p(t) - f_p^*(t))^2 \quad (20)$$

#### Subject to

- (7–12)
- (13) or (14)
- (17–19)

where  $T$  is the set of time points,  $f_p(t)$  and  $f_p^*(t)$  are the estimated and the desired concentration of a protein  $p$  at a time point  $t$ .

### Results

Both the steady-state and the temporal profile optimization problems can be solved by using global mixed-integer non-linear solvers that rely on linearization, convexification, and application of branch and bound methods. Here, we used the COUENNE 0.4.0 open-source platform [21], which we extended in scope to handle the problems that we focus on: we decoupled termination conditions for the primal-dual gap, and modified the updating condition in the bound tightening procedure by introducing threshold parameters. To evaluate the capacity of our optimization framework to yield synthetic circuits with the desired characteristics, we assessed its performance in three synthetic circuits that have been constructed experimentally: a band detector system [22–23], a transcriptional cascade [24], and a toggle switch [25]. For all designs, we used parameter values that were previously reported in literature (Table 1), and the initial protein concentrations were assumed to be zero. Regarding the experimentally characterized part mutant libraries that we used [26–28], all promoter mutants differ in their basal level of production  $\alpha_{0k}$  and the protein synthesis coefficient  $\alpha_k$ . In order to evaluate the scalability of the framework, we constructed synthetic

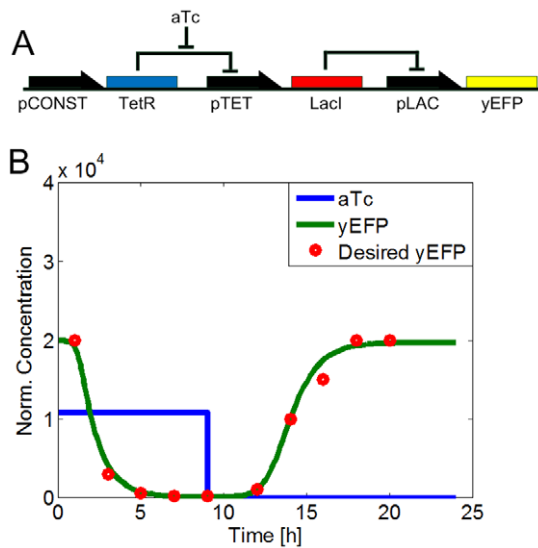


**Figure 3. Transcriptional cascade design.** A) The system is controlled by the inducer aTc which can bind to TetR and reduce the concentration of free TetR molecules. This concentration change will be propagated through the cascade to the change of the reporter yEFP. B) Temporal profile of a cascade design: The desired output (yEFP, red dots) and the actual output (green line) of the optimal synthetic gene circuit are shown. The temporal profile was split into two phases, based on changes in the inducer concentration. In the first phase (0 h–9 h), 2.16 μM aTc (blue line) is added and in the second phase (9 h–24 h) aTc is washed out (setting as the experiment in [24]). doi:10.1371/journal.pone.0035529.g003

libraries that consisted of synthetic promoter parts with parameter values within the experimentally measured range, with a sampling distribution that varied from uniform to gamma (more details below).

### Band Detector Design

We used the MINLP optimization framework to find the optimal combination of promoters for a six-promoter bandpass design that acts as a filter: the output is high only when the input is within a specific range or “band”. The first bandpass synthetic design was used to detect acyl-HSL signal in a population of bacteria [22–23]. In [12], a simpler design to detect L-arabinose within a bacterium was introduced (Fig. 2A). The mode of operation for this circuit is the following: The output, a GFP reporter protein is only high when TetR protein is not present. There are two pathways that produce TetR, one directly through activation of the pBAD promoter, and another through the LacI de-repression of the Lac promoter. When the concentration of L-arabinose is high, L-arabinose will bind to AraC and prevent it binding to pBAD and repress its expression. This results in TetR expression through the pBAD-TetR pathway. At the same time, LacI will also be expressed and it will repress the pLAC-TetR production pathway. Similarly, the opposite is observed at low concentrations of L-arabinose, where the pLAC-TetR pathway is activated and the pBAD-TetR pathway repressed. Therefore, TetR will be expressed for both cases: low or high concentration of L-arabinose. However, because of the difference in the regulation of pBAD and pLAC, there will be a value interval of L-arabinose that the expression level of TetR is low, and the GFP reporter protein is expressed (Figure 2A).

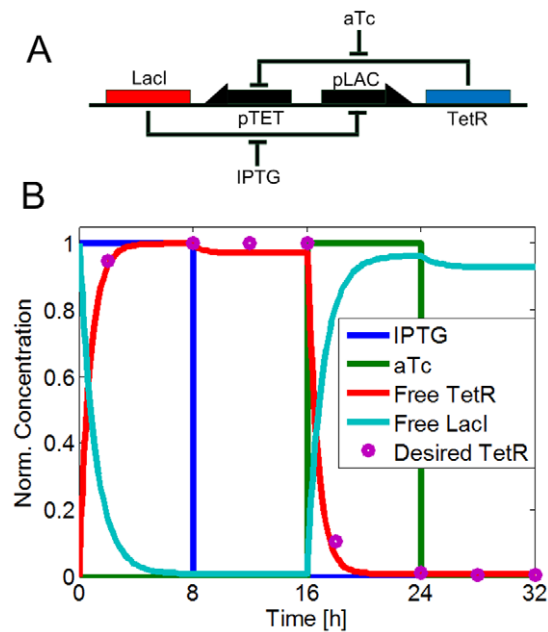


**Figure 4. Toggle switch design, where two genes (LacI and TetR) negatively regulate each other.** A) The system is externally controlled through the addition of two inducers, IPTG and aTc, which bind to the repressors and decrease their regulatory potential. B) Expression profile of the resulting synthetic circuit: The desired profile (input, depicted with purple dots) and actual profile (red line) for the TetR protein is shown. The temporal profile was split into four phases, based on changes in the inducer concentrations. Phase 1: IPTG high, aTc low; Phase 2: IPTG low, aTc low; Phase 3: IPTG low, aTc high; Phase 4: IPTG low, aTc low. doi:10.1371/journal.pone.0035529.g004

A dataset with experimentally characterized promoters [27–29] of various strengths and types (constitutive, pBAD, LacI, TetR) was used as the library of parts available. Model parameters were set on literature reported values for *E. coli* and are summarized in Table 1. In the original band-detector circuit, the objective function is a steady-state I/O characteristic between the input (inducer L-arabinose) and the output (reporter GFP), with no specification on the transient characteristics of the system. The MINLP optimization method was able to find the optimal combination of parts for the steady-state case within minutes (Figure 2B). Similar results were obtained for temporal profile optimization at a L-arabinose concentration of 30 mM by using the linear model described above (Fig. 2C). The optimality of the solution was verified by running exhaustive search.

### Transcriptional cascade design

Next, we used the MINLP optimization framework to identify optimal part combinations for the temporal profile of a transcriptional cascade design that was proposed in [24]. According to this design, TetR is under a constitutive promoter and it represses LacI expression, which in turns represses yEFP. (Fig. 3A). At normal conditions, TetR will be created and bind to the pTET promoter to prohibit LacI production and thus the expression level of yEFP is high. When the inducer aTc is added, this inducer will bind to TetR proteins and prevent them binding to the pTET promoter and thus the production of LacI from this promoter will be maximized and the expression level of yEFP is low. If the inducer aTc is washed away, the system returns to the initial condition and the expression level of yEFP is high.



Previously, we used the promoter library from [26] and [27] as inputs to our optimization framework. The time course is divided into 2 phases, based on the presence of the inducer aTc. The characteristic function of the resulting optimal design is showed in figure 3B.

### Toggle switch design

Toggle switches, also known as flip-flops, are fundamental memory blocks that have two stable attractor points, where one of the outputs is high and the other is low. As a test case we used the toggle switch design from [25]. As shown in figure 4A, the design has two genes, LacI and TetR, that negatively regulate each other. This is possible through the addition of a LacI promoter in front of the TetR gene (denoted as pLAC), and a TetR promoter in front of the LacI gene (denoted as pTET). In addition, the system can be controlled by the chemical inducers IPTG and aTc that can shut down the repressing effect of LacI and TetR, respectively.

The toggle switch has two-attractor dynamics, as shown in Figure 4B: The system initially is in one of the two steady states, with either LacI or TetR overexpressed. When the system is induced with IPTG, the inducer binds to LacI and it suppresses its regulatory activity upon the TetR production (phase 1). This leads to the overexpression of TetR gene (which is now de-repressed, in the absence of LacI), that in turn shuts down the LacI production, by binding to its promoter and acting as a repressor. So, even when IPTG is washed away from the system (phase 2), LacI remains repressed. Subsequent addition of the aTc inducer results to its binding to TetR protein, changing its conformation and thus, de-repressing the LacI protein, which now is free to start repressing the TetR expression (phase 3). Once this reaches a steady state, it remains at that state, even at the removal of the inducer aTc (phase 4). A mutant library for the Tet and Lac promoters was used as before [26]. The objective function was set to be the transient dynamics of a toggle switch with respect to the TetR protein, as shown in figure 4B. As discussed in the methods section, in order to better approximate the temporal profile of this circuit, its profile was split in four phases as dictated by the various inducer concentrations.

### Method evaluation: approximation error, running time and scalability analysis

**Approximation error and running time.** Table 2 summarizes the approximation error and running time of exhaustive search (ES), a genetic algorithm heuristic (GA) and the proposed mixed-integer non-linear programming (MINLP) approach on all three design problems. To increase the likelihood that the GA will find the globally optimal solution, we performed a number of initial point randomizations and kept the heuristic running time within the same order of magnitude as the MINLP method. For the latter, we allowed the solution to be near-optimal with a duality gap (i.e., a guaranteed upper bound on the approximation error) of less than  $10^{-7}$ . As it is shown in Table 2, both the GA and MINLP method were able to find optimal or near-optimal solutions much faster than exhaustive search. In addition, MINLP outperforms the GA heuristic in all steady-state cases, and it performs on par or better in all temporal optimization cases. However, we stress again that the major advantage of MINLP is that it can *guarantee* the optimality of the solution, or its maximum deviation from such optimal point, something that heuristics are unable to provide.

**Scalability and sensitivity analysis.** In order to measure the scalability of MINLP approach, we have evaluated it on the cascade design with different input library sizes as in figure 5. As shown in the table, the ratio between ES to MINLP running time increases considerably as the library size scales up. In addition, since the MINLP problem is solved by a branch-and-bound algorithm, the distribution of part values may affect the running time of the algorithm. To check the sensitivity of our MINLP framework on the distribution of parts in the library, we generated three synthetic libraries. In the first, the part values were uniformly distributed within the parameter range. In the second, the parts were gamma distributed with a mean near the parameters of the optimal solution (identified by the previous experiment). Similarly, in the third library, the part values are gamma distributed with a mean that is far from the optimal part parameters. As it is evident from figure 5, high density of parts in the region of the optimal solution leads to inferior performance (about an order of magnitude for all library sizes), since the existence of many near-

**Table 2.** Comparison of the approximation error and running time.

Design	Library	Running	Optimal	Running	$\Delta$ Error	$\Delta$ Error	Running	$\Delta$ Error
	Size	Time	Error	Time	Min	Max	Time	Final
		(ES)	(ES)	(GA)	(GA)	(GA)	(MINLP)	(MINLP)
Band detector								
Steady state	$10^6$	$1.2 \times 10^4$	$1.3 \times 10^{-2}$	$1.2 \times 10^3$	0	$1.9 \times 10^{-1}$	$1.5 \times 10^3$	0
Temporal	$10^6$	$5.0 \times 10^4$	$3.3 \times 10^{-4}$	$2.0 \times 10^3$	$1.0 \times 10^{-5}$	$2.3 \times 10^{-2}$	$2.0 \times 10^3$	$1.6 \times 10^{-3}$
Cascade								
Steady state	$100^3$	$7.3 \times 10^3$	$3.8 \times 10^{-7}$	$8.2 \times 10^1$	$5.6 \times 10^{-6}$	$1.4 \times 10^{-3}$	$7.1 \times 10^1$	$4.0 \times 10^{-6}$
Temporal	$100^3$	$8.7 \times 10^3$	$1.5 \times 10^{-2}$	$1.2 \times 10^2$	0	$1.5 \times 10^1$	$1.8 \times 10^2$	$4.4 \times 10^{-3}$
Toggle Switch								
Steady state	$1000^2$	$2.5 \times 10^4$	$8.2 \times 10^{-4}$	$1.0 \times 10^3$	$3.2 \times 10^{-3}$	$4.7 \times 10^{-1}$	$9.9 \times 10^2$	0
Temporal	$1000^2$	$3.2 \times 10^4$	$1.8 \times 10^{-3}$	$1.3 \times 10^2$	0	$5.0 \times 10^{-1}$	$7.7 \times 10^3$	$1.7 \times 10^{-2}$

A comparison of the running time (seconds) and the optimality of the exhaustive search (ES) method, the genetic algorithm (GA) heuristic and the proposed mixed-integer non-linear programming approach (MINLP). "Optimal error" refers to the squared difference between the desired protein value and the optimal circuit value, when the latter was found through exhaustive search. "Error" refers to the difference between the optimal error and the heuristic or MINLP error. Since the genetic algorithm solution depends on the initial conditions, "Error Min" and "Error Max" are given.

doi:10.1371/journal.pone.0035529.t002



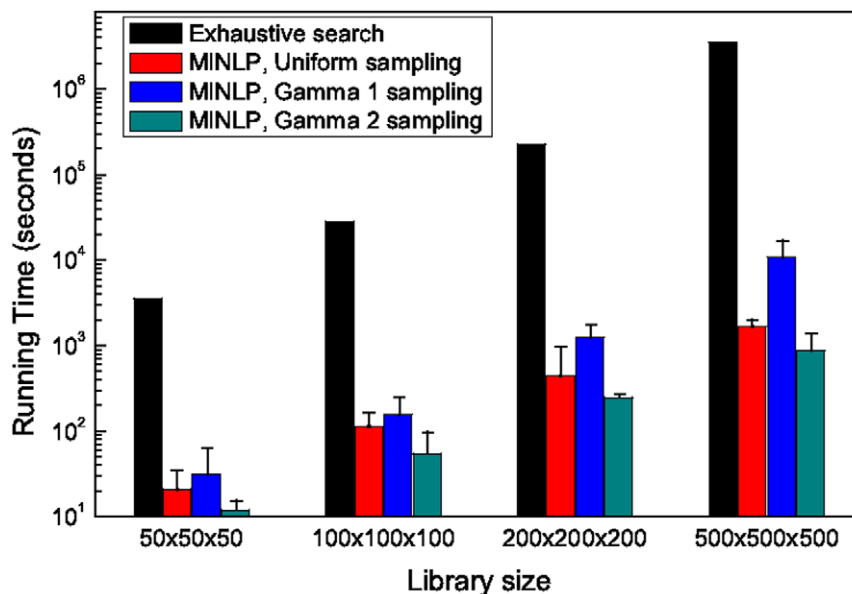


**Figure 5. Scalability and sensitivity of the running time of the MINLP approach on different inputs.** A comparison of the running time (seconds) of the MINLP approach on different input sizes and different data input distribution for the steady state cascade design problem (5 synthetic datasets per case). Parameter values are generated by sampling within the parameter range that has been experimentally measured [26–27]. Samples are distributed either uniformly (uniform sampling), following a gamma distribution with the mean set on the optimal set parameter values (Gamma 1 sampling), or away from that mean (Gamma 2 sampling). The running time of exhaustive search method (ES) is estimated for the last library size.

doi:10.1371/journal.pone.0035529.g005

optimal solutions render the branch-and-bound task difficult. Similarly, the inverse is observed when the part values are not close to the optimal solution. Nevertheless, the performance of the algorithm was in all cases orders of magnitude better than the exhaustive case.

## Discussion

In this paper we introduced a global mixed-integer non-linear programming framework for the automatic construction of synthetic gene circuits with either steady-state or temporal objectives. Profiling, scalability and sensitivity analysis on three synthetic circuits that have been experimentally constructed in the past, show that the method compares favorably to both exhaustive search and heuristic methods. In addition, in contrast to all other techniques so far, the method presented is able to provide guarantees on the global optimality of the solution.

There are several extensions of this work that warrant further investigation. First, we will systematically investigate how the circuit topology affects the performance of this and other methods. Although our results were similar for all three topologies that we analyzed, we expect that the topological characteristics of the synthetic circuits (e.g., the number of feedback loops present) together with the parameter distribution of the parts library will play a significant role on the performance of any automatic circuit construction method. In addition, we can extend the current framework to include in the optimal set of other part types (operator sites, ribosomal binding sites, gene mutants, etc.) during

the optimization procedure. Although we are currently lacking well-characterized libraries of such components, recent initiatives (such as the Biofab project) will increase the availability of such components. One formidable technical challenge is to come up with an automatic way to determine the threshold values that are related to the optimization method and tools used. For example, COUENNE uses an error threshold for bound tightening that we found to have significant effect on the number of infeasible cases that the tool reports. By adjusting this threshold we were able to decrease the number of infeasible cases to zero, at the cost of computational time. Currently there is no way to estimate the threshold value, and an adaptive iterative method may produce interesting results. Finally, the proposed framework can be extended towards *ab initio* synthetic circuit design where the circuit topology is not known. The method presented here, provides a stepping stone towards building highly efficient, pragmatic tools for synthetic circuit design.

## Acknowledgments

We would like to thank members of the Tagkopoulos Lab for the comments and helpful discussions.

## Author Contributions

Conceived and designed the experiments: LH MK JK IT. Performed the experiments: LH. Analyzed the data: LH MK IT. Wrote the paper: LH MK IT.

## References

- Lu T, Collins J (2009) Engineered bacteriophage targeting gene networks as adjuvants for antibiotic therapy. *Proc Natl Acad Sci USA* 106: 4629.
- Mukhopadhyay A, Redding A, Rutherford B, Keasling J (2008) Importance of systems biology in engineering microbes for biofuel production. *Current opinion in biotechnology* 19: 228–234.
- Marchisio MA, Stelling J (2011) Automatic design of digital synthetic gene circuits. *PLoS Comput Biol* 7: e1001083.
- Pedersen M, Phillips A (2009) Towards programming languages for genetic engineering of living cells. *Journal of The Royal Society Interface* 6: S437–S450.

5. Densmore D, Kittleston J, Bilitchenko L, Liu A, Anderson J (2010) Rule based constraints for the construction of genetic devices. In: Circuits and Systems (ISCAS), Proceedings of 2010 IEEE International Symposium on. IEEE. pp 557–560.
6. Beal J, Lu T, Weiss R (2011) Automatic compilation from high-level biologically-oriented programming language to genetic regulatory networks. PLoS ONE 6: e22490.
7. Francois P, Hakim V (2004) Design of genetic networks with specified functions by evolution in silico. Proc Natl Acad Sci USA 101: 580–585.
8. Wu CH, Lee HC, Chen BS (2011) Robust synthetic gene network design via library-based search method. Bioinformatics 27: 2700–2706.
9. Rodrigo G, Carrera J, Jaramillo A (2007) Genetdes: automatic design of transcriptional networks. Bioinformatics 23: 1857–1858.
10. Rodrigo G, Carrera J, Jaramillo A (2011) Computational design of synthetic regulatory networks from a genetic library to characterize the designability of dynamical behaviors. Nucleic acids research 39: e138.
11. Feng XJ, Hooshangi S, Chen YD, Li YG, Weiss R, et al. (2004) Optimizing genetic circuits by global sensitivity analysis. Biophysical Journal 87: 2195–2202.
12. Dasika M, Maranas C (2008) OptCircuit: an optimization based method for computational design of genetic circuits. BMC Systems Biology 2: 24.
13. Goodwin B (1965) Oscillatory behavior in enzymatic control processes. Advances in Enzyme Regulation 3: 425–437.
14. Griffith JS (1968) Mathematics of cellular control processes i. negative feedback to one gene. Journal of Theoretical Biology 20: 202–208.
15. Griffith JS (1968) Mathematics of cellular control processes ii. positive feedback to one gene. Journal of Theoretical Biology 20: 209–216.
16. Weiss JN (1997) The hill equation revisited: uses and misuses. The FASEB journal official publication of the Federation of American Societies for Experimental Biology 11: 835–841.
17. Bansal V, Sakizlis V, Ross R, Perkins JD, Pistikopoulos EN (2003) New algorithms for mixedinteger dynamic optimization. Computers & Chemical Engineering 27: 647–668.
18. Boyce WE, DiPrima RC (2009) Elementary Differential Equation and Boundary Value Problem. Wiley, New York.
19. Bellman RE (1953) Stability Theory of differential Equations. McGraw-Hill, New York.
20. Moler C, Loan CV (2003) Nineteen dubious ways to compute the exponential of a matrix, twentyfive years later. SIAM REVIEW. pp 3–49.
21. Belotti P, Lee J, Liberti L, Margot F, Waechter A (2009) Branching and bounds tightening techniques for non-convex MINLP. Optimization Methods and Software 24: 597–634.
22. Basu S, Karig D, Weiss R (2002) Engineering signal processing in cells: Towards molecular concentration band detection. In: DNA Computing. pp 61–72.
23. Basu S, Gerchman Y, Collins CH, Arnold FH, Weiss R (2005) A synthetic multicellular system for programmed pattern formation. Nature. pp 1130–1134.
24. Hooshangi S, Thiberge S, Weiss R (2005) Ultrasensitivity and noise propagation in a synthetic transcriptional cascade. Proc Natl Acad Sci USA 102: 3581–3586.
25. Gardner T, Cantor C, Collins J (2000) Construction of a genetic toggle switch in *Escherichia coli*. Nature 403: 339–342.
26. Ellis T, Wang X, Collins J (2009) Diversity-based, model-guided construction of synthetic gene networks with predicted functions. Nature biotechnology 27: 465–471.
27. Berkeley 2006 iGEM Team. Constitutive promoter family (Retrieved May, 2011). <http://partsregistry.org/Promoters/Catalog/Anderson>.
28. British-Columbia 2009 iGEM Team. pBAD promoter family (Retrieved May, 2011). [http://partsregistry.org/PBAD\\_Promoter\\_Family](http://partsregistry.org/PBAD_Promoter_Family).
29. Davis JH, Rubin AJ, Sauer RT (2011) Design, construction and characterization of a set of insulated bacterial promoters. Nucleic acids research 39: 1131–1141.
30. Braun, Basu S, Weiss R (2005) Parameter estimation for two synthetic gene networks: a case study. In: IEEE International Conference on Acoustics, Speech, and Signal Processing. pp 769–772.
31. Kuhlman T, Zhang Z, Saier MH, Hwa T (2007) Combinatorial transcriptional control of the lactose operon of *Escherichia coli*. Proc Natl Acad Sci USA 104: 6043–6048.
32. García-Ojalvo J, Elowitz M, Strogatz S (2004) Modeling a synthetic multicellular clock: Repressilators coupled by quorum sensing. Proc Natl Acad Sci USA. pp 10955–10960.
33. Elowitz MB, Leibler S (2000) A synthetic oscillatory network of transcriptional regulators. Nature. pp 335–338.
34. Tuttle LM, Salis H, Tomshine J, Kaznessis YN (2005) Model-driven designs of an oscillating gene network. Biophysical Journal 89: 3873–3883.
35. Nath K, Koch AL (1970) Protein degradation in *Escherichia coli*: I. measurement of rapidly and slowly decaying components. Journal of Biological Chemistry 245: 2889–2900.
36. Rachael, Wadler C, John (2002) Long-term and homogeneous regulation of the *Escherichia coli* araBAD promoter by use of a lactose transporter of relaxed specificity. Proc Natl Acad Sci USA. pp 7373–7377.